Nanoscale Advances

ROYAL SOCIETY OF CHEMISTRY

COMMUNICATION

View Article Online
View Journal | View Issue

Cite this: *Nanoscale Adv.*, 2022, **4**, 387

Received 24th September 2021
Accepted 26th November 2021

DOI: 10.1039/d1na00711d

rsc.li/nanoscale-advances

Impurities in polyvinylpyrrolidone: the key factor in the synthesis of gold nanostars†

Patricia Taladriz-Blanco, [ac] Miguel Spuch-Calvar,‡[a] Anselmo del Prado, §[a] Christoph Weder, [a] Barbara Rother-Rutishauser, [a] Alke Petri-Fink *[ab] and Laura Rodriguez-Lorenzo *[c]

Control over the synthesis of anisotropic nanoparticles is crucial as slight differences in their size, shape, sharpness, or the number of tips in the case of gold nanostars, has an inordinate influence on their properties and functionality for future applications. Herein, we show that the supplier and purity of polyvinylpyrrolidone (PVP) can significantly alter the synthesis of gold nanostars, demonstrating that impurities, not PVP itself, are the main factor responsible for star-like shape formation. We demonstrate that in the presence of pure PVP and *N*,*N*-dimethylformamide, the use of hydrazine leads to the formation of branched nanoparticles. This synthetic approach opens the door to solving issues associated with the use of commercial PVP during the synthesis of gold nanostars.

Introduction

Gold (Au) nanostars (NSTs) are one of the most promising anisotropic nanoparticles (NPs) for sensing and imaging. High sensitivity detection is facilitated by concentration of the electromagnetic field at their tips, thus enhancing *e.g.* the Raman signal of the molecules subject to study and facilitating their detection.[1,2] In this regard, Au NSTs are preferred candidates for the detection of multiple analytes by surface-enhanced Raman scattering (SERS), including bacteria,[3] biomarkers,[4,5] nucleic acids,[6] organic and inorganic[7–11] molecules.

The precise control of the sharpness (*i.e.* length and angle) and the number of tips in nanostars allows tuning the concentration of the electromagnetic field at the tips and therefore their performance as optical nanoantennas for the induction of SERS.[2,12–15]

Recently, the presence of impurities in commercial chemicals has drawn scientists' attention, as it has become clear that those impurities can play an important role on the syntheses of NPs. In this context, Roger *et al.*[16] demonstrated that the presence of impurities in polyvinylpyrrolidone (PVP) drastically influences the synthesis of silver NPs. Rioux *et al.*[17] demonstrated that the PVP end-groups play a pivotal role in the synthesis of anisotropic NPs. The authors found that aldehyde PVP end-groups (PVP-CHO) lead to the formation of silver nanocubes, whereas PVP-OH and PVP-H yield a mixture of particles having different shapes. Warned by colleagues who observed that only one of the two PVP grades used during their experiments prevented the aggregation of Ag NPs upon dilution, Sacher *et al.*[18] characterized the two PVPs purchased from the same supplier. The authors concluded that the commercial PVP used in the study contained 2-pyrrolidone and hydroperoxides as contaminants. In a recent editorial, Liz-Marzán *et al.*[19] recommended considering impurities when synthesizing NPs, pointing out that the use of different commercial PVPs influences the reaction time required for the reduction of Au^{3+} into Au^{+} as well as the time needed to grow Au NSTs. In 2008, the same author published a protocol to synthesize Au NSTs[20] that yields well-defined NSTs (reaction yield ~100%) with high colloidal stability and biocompatibility using PVP. The reported synthesis is carried out at room temperature without any external stimulus (*e.g.* light) and involves the reduction of a chloroauric acid ($HAuCl_4$) in the presence of *N*,*N*-dimethylformamide (DMF), PVP, and 15 nm PVP-coated gold spherical seeds. In this reaction, DMF acts as both the solvent and the reducing agent, and in the presence of metal seeds and at high concentrations of PVP (>2.5 mM) Au^{3+} is

[a]*Adolphe Merkle Institute, University of Fribourg, Chemin des Verdiers 4, Fribourg, CH-1700, Switzerland. E-mail: alke.fink@unifr.ch*

[b]*Chemistry Department, University of Fribourg, Chemin du Musée 9, Fribourg, CH-1700, Switzerland*

[c]*International Iberian Nanotechnology Laboratory (INL), Water Quality group, Av. Mestre José Veiga s/n, 4715-330 Braga, Portugal. E-mail: laura.rodriguez-lorenzo@inl.int*

† Electronic supplementary information (ESI) available. See DOI: 10.1039/d1na00711d

‡ Present address: Department of Applied Physics, Department of Physical Chemistry, Singular Center for Biomedical Research (CINBIO), Southern Galicia Institute of Health Research (IISGS) and Biomedical Research Networking Center for Mental Health (CIBERSAM), Universidade de Vigo, 36310 Vigo, Spain.

§ Present address: Departamento de Química Orgánica, Facultad de Ciencias, Universidad Autónoma de Madrid, 28049 Madrid, Spain.

reduced to Au^0 to grow on the surface of the metal seeds.[21,22] The anisotropic growth in the [011] direction is driven by PVP, which is preferentially adsorbed on specific facets of the gold seeds and is responsible for the control of the nucleation kinetics.[23] Furthermore, PVP chains provide colloidal stability to the formed stars.[22]

In the synthesis of Au NSTs, the role of PVP and DMF as well as temperature, size and crystallinity of the seed, or proton (H^+) addition (*i.e.* presence of HCl) among others were already studied[12,14,20,21,23,24] However, to the best of our knowledge, the impact of the presence of impurities in the PVP during the synthesis of Au NSTs has not been yet addressed. Following the protocol described by Liz-Marzán to synthesize Au NSTs with PVP,[20] we demonstrate that the use of PVP from different suppliers with different purity compromises the anisotropic growth of the Au NPs. In addition, our results show that the purification of PVP drastically suppresses the formation of Au NSTs independent on its molecular weight. Finally, we explore the influence of hydrazine in the synthesis of Au NSTs using purified PVP with two different molecular weights, 10k and 40k, observing that the presence of hydrazine leads to the formation of branched NPs.

Alternatives to using PVP include the use of surfactants (such as cetyltrimethylammonium bromide[25] or Triton[26]), buffers (*e.g.* HEPES[27]) or silver nitrate in acidic pH to induce the anisotropic growth[28] among others.[29]

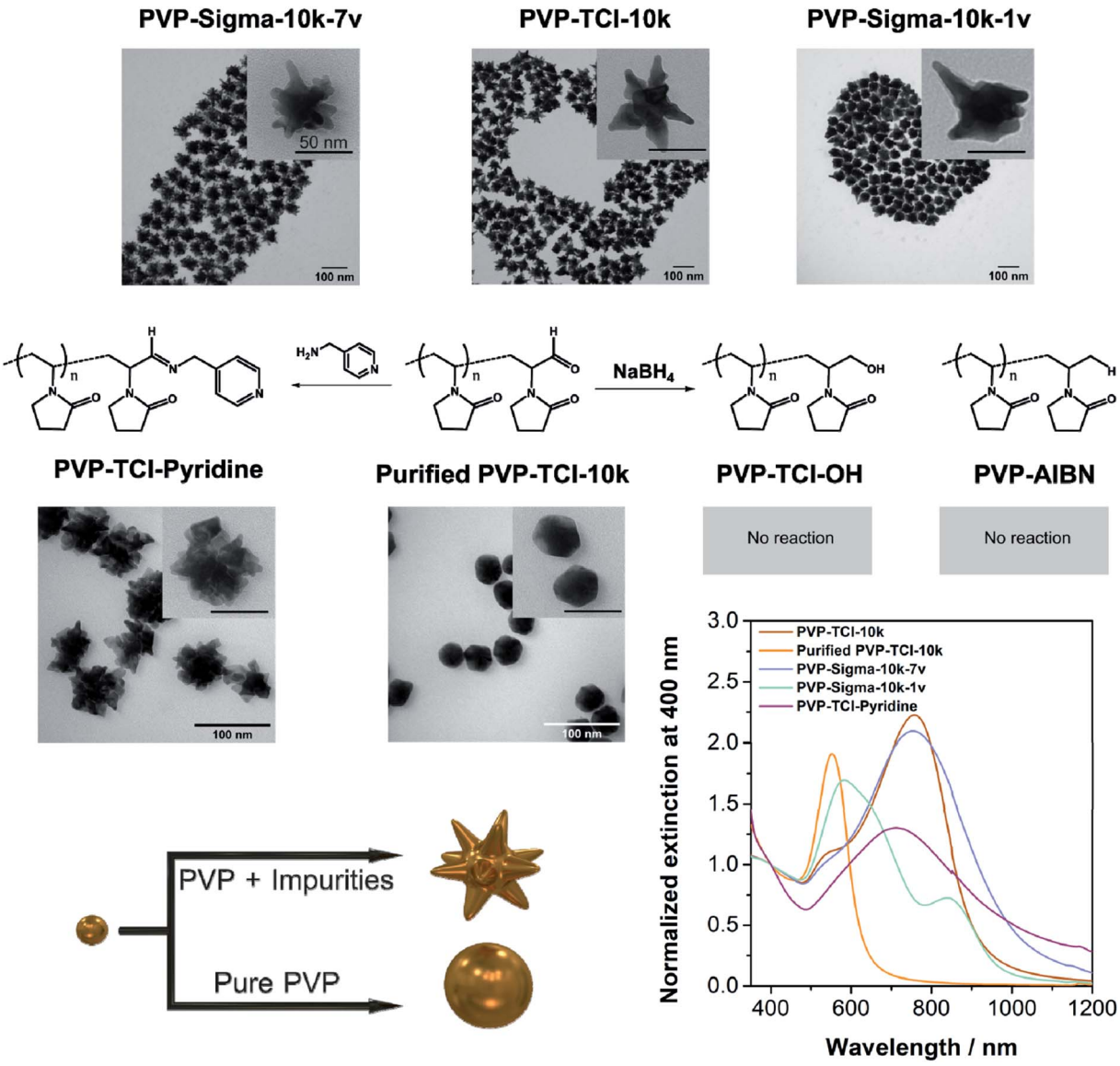

Fig. 1 Schematic representation of the PVPs used in this study, TEM micrographs, and extinction spectra of the Au NPs that were synthesized in the presence of different PVPs. Top row: Au NSTs synthesized in the presence of two different lots of PVP supplied by Sigma-Aldrich (PVP-Sigma-10k-7v and PVP-Sigma-10k-1v), and PVP supplied from TCI (PVP-TCI-10k). Middle row: Au NSTs synthesized in the presence of purified PVP supplied by TCI (Purified PVP-TCI-10k), purified PVP-TCI-10k pyridine end-terminated (PVP-TCI-pyridine), purified PVP-TCI-10k hydroxyl-end terminated (PVP-TCI-OH), and PVP prepared in our laboratories using AIBN as an initiator (PVP-AIBN). The 3D sketch represents the relevance of the impurities on the formation of Au NSTs.

Results and discussion

Au NSTs in the presence of three commercial PVPs (M_w = 10 kDa), PVP-TCI-10k (Lot 48NUD-DE), PVP-Sigma-10k-7v (Lot BCBM0097V), and PVP-Sigma-10k-1v (Lot BCBG5331V), respectively were prepared following the protocol described by Liz-Marzán *et al.*[20] The results indicate that all PVPs used in our study lead to the formation of anisotropic Au NPs. Transmission electron microscopy (TEM) micrographs in Fig. 1 show that the Au NSTs prepared using PVP-TCI-10k are well-defined and exhibit large and sharp tips, while the Au NSTs prepared using PVP-Sigma-10k-7v have shorter and rounded tips. The morphology of the Au NSTs prepared with PVP-Sigma-10k-1v is ill-defined with a low number of rounded tips. The extinction spectra of the synthesized Au NSTs (Fig. 1) show that the tip-mode plasmon resonance band of PVP-Sigma-10k-7v (blue spectrum) is broader than the tip-mode band of the PVP-TCI-10k (red spectrum), which agrees with the higher number of shorter tips with a higher aperture angle in PVP-Sigma-10k-7v as visualized in the TEM micrographs. The localized surface plasmon resonance (LSPR) band corresponding to core mode resonance is predominant in the UV-Vis-NIR spectrum of PVP-Sigma-10k-1v (cyan spectrum) due to the lack of tips observed in TEM micrograph. The three PVPs were characterized by ^{1}H-NMR spectroscopy (Fig. 2), which demonstrates the presence of impurities in PVP-TCI-10k (spectrum A) and PVP-Sigma-10k-7v (spectrum E), but not in PVP-Sigma-10k-1v (spectrum D).

Based on the hypothesis that the purity of PVP strongly influences the synthesis of Au NSTs, commercial PVP-TCI-10k was purified by precipitation from chloroform into diethyl ether (see details in the ESI section Material and Methods†) which gives rise to NPs with a low degree of anisotropy (Fig. 1). The presence of impurities is drastically suppressed by this purification (Fig. 2), as shown by ^{1}H-NMR spectra of PVP-TCI-10k before and after purification. This result was confirmed by analyzing the ^{1}H-NMR spectrum of the fraction isolated from the supernatant after the precipitation step (Fig. 2). The broad distribution of masses detected by Matrix Assisted Laser Desorption/Ionization-Time of Flight Mass Spectrometry (MALDI-TOF) (Fig. S1†) of the supernatant fraction confirms the presence of PVP oligomers, as previously reported.[30] Thus, in case of PVP-TCI-10k, PVP oligomers, which can be considered as an impurity, may serve to promote the formation of Au NSTs.

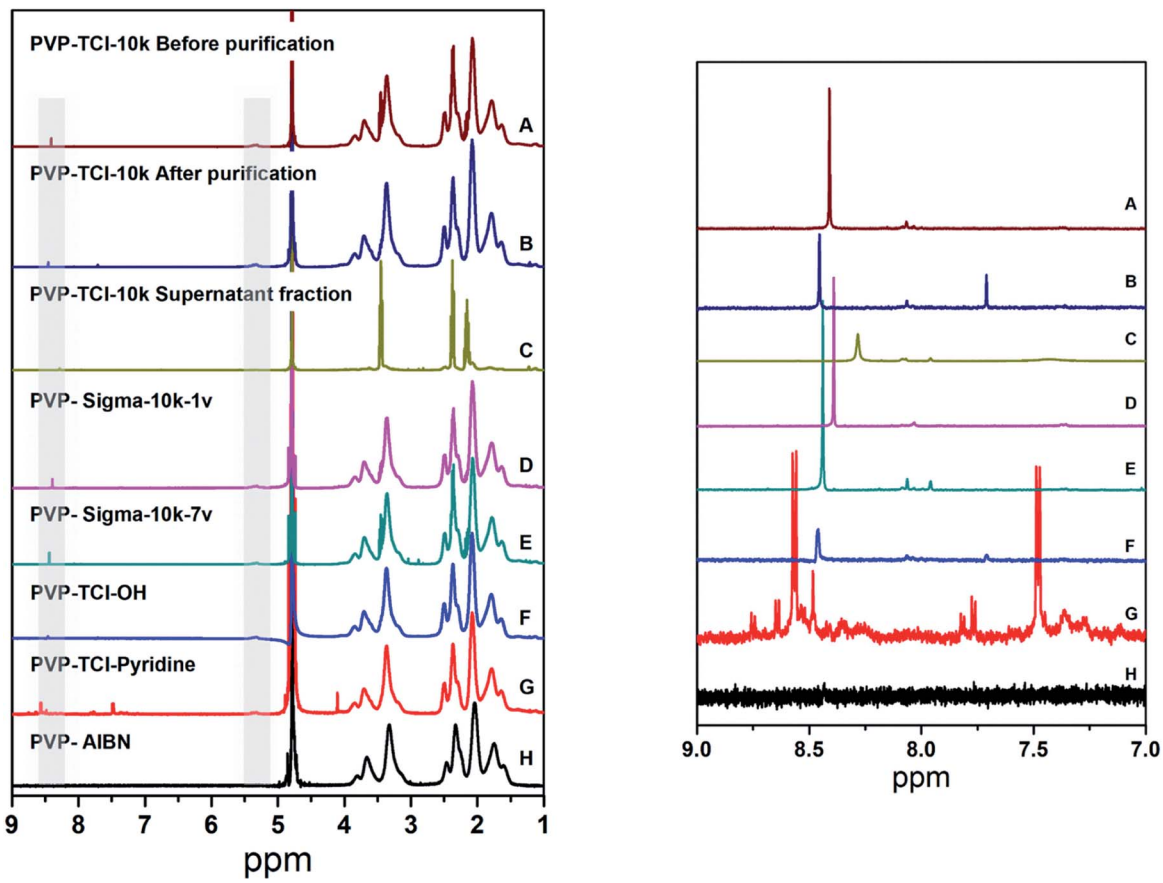

Fig. 2 Left: ^{1}H-NMR spectra of PVP-TCI-10k before (A) and after (B) purification by precipitation. (C) ^{1}H-NMR spectra of the supernatant fraction recovered after precipitating PVP-TCI-10k, (D) PVP-Sigma-10k-1v, and (E) PVP-Sigma-10k-7v. ^{1}H-NMR spectra of purified PVP-TCI-10k hydroxyl end-terminated (F, PVP-TCI-OH), and pyridine end-terminated (G, PVP-TCI-pyridine). ^{1}H-NMR spectra of PVP synthesized in our laboratories using AIBN as an initiator (H, PVP-AIBN). Dashed vertical black lines indicate signals associated with oligomers and the presence of an aldehyde end group. Right: Spectra zoom view from 7 to 9 ppm. All spectra were taken in D_2O at 25 °C.

All NMR spectra show a peak at *ca.* 8.5 ppm and a weak band at *ca.* 5.2 ppm corresponding to alpha –CH– groups, suggesting the presence of aldehyde end groups. Diffusion Ordered Spectroscopy (DOSY) NMR data confirms that these residues are part of the PVP chains (Fig. S1†).

In contrast to what has been previously reported,[31,32] no hydroxyl end groups were identified in the as-received and purified PVP-TCI-10k by ^{1}H-NMR spectroscopy (Fig. 2) due to signal overlap from the PVP backbone which possesses broad signals in the region of 3–4 ppm.

As described by Straub *et al.*,[33] the synthesis of commercial PVP often relies on hydrogen peroxide as an initiator, and this leads to the introduction of hydroxyl end groups, which may oxidize into aldehyde groups.[18] In our study, the presence of aldehyde end groups, as suggested by the ^{1}H-NMR data discussed above, was further confirmed by (1) reducing the purified PVP-TCI-10k with $NaBH_4$ forming a hydroxyl end-terminated PVP (PVP-TCI-OH), and (2) reacting the purified PVP-TCI-10k with 4-aminopyridine (PVP-TCI-pyridine), respectively. As shown in the ^{1}H-NMR spectra and more clearly by DOSY, the treatment of purified PVP-TCI-10k (Fig. 2 and S2†) with $NaBH_4$ leads to the disappearance of the bands at 8.5 and 5.2 ppm, confirming the reduction of PVP-CHO to PVP-OH. The pyridine coupling *via* imine formation is confirmed by the

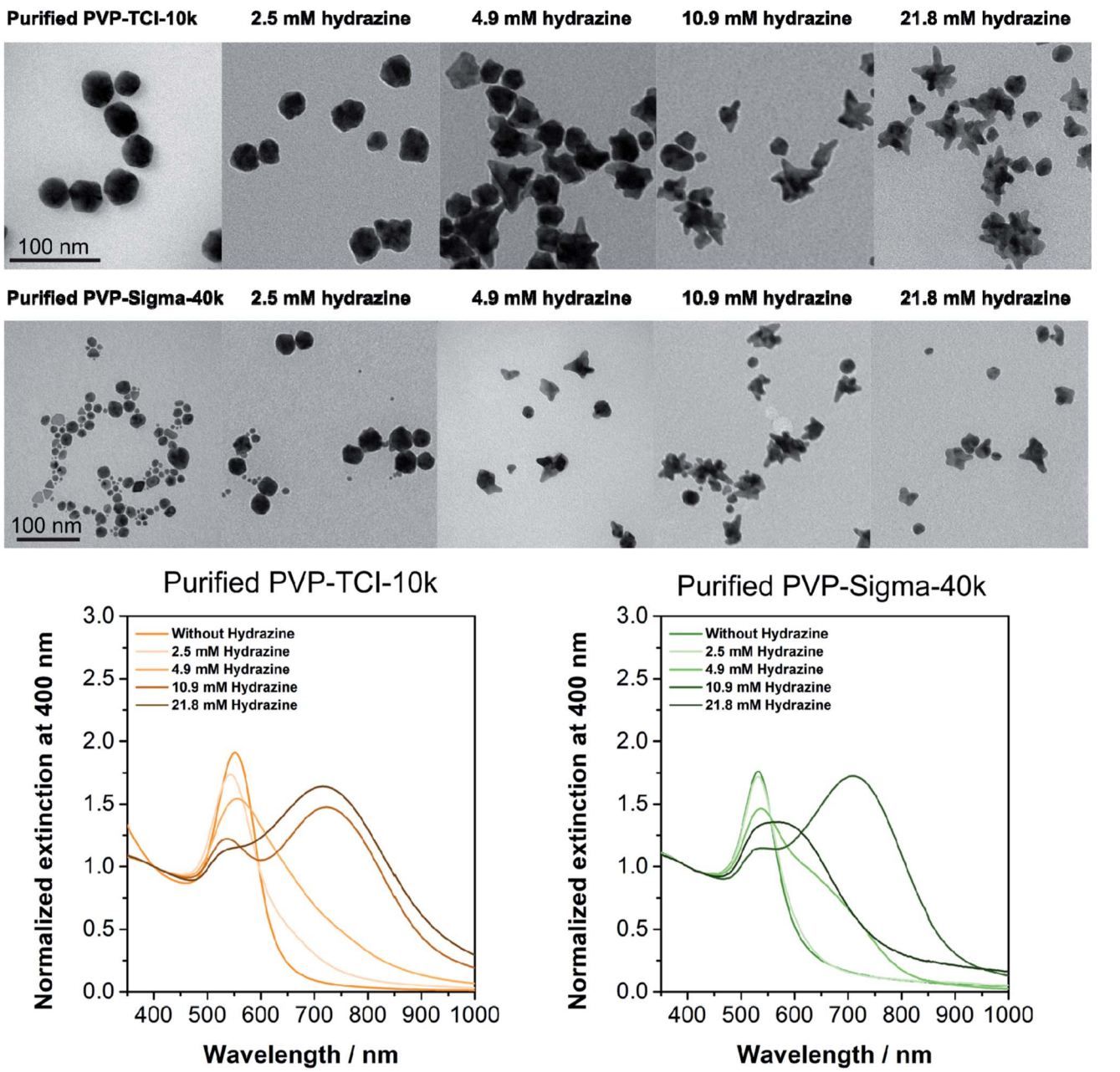

Fig. 3 TEM micrographs and extinction spectra showing the influence of hydrazine in the synthesis of Au NSTs using purified commercial PVP-TCI-10k and PVP-Sigma-40k. Despite the lower yield and the high polydispersity of the synthesis, the use of hydrazine leads to the formation of branched NPs.

appearance of two new peaks at 7.5 and 8.5 ppm corresponding to the pyridine group (Fig. 2).

Contrary to what was described by Xia *et al.*,[32,34] no reaction was observed in attempts to produce NPs in the presence of PVP-TCI-OH (Fig. 1 and S3A†). Therefore, hydroxyl end groups in the PVP chain can neither be responsible for the reduction of the gold salt nor for the anisotropic growth. NPs synthesized in the presence of PVP-TCI-pyridine exhibit a more significant anisotropic growth than those prepared with the purified PVP-TCI-10k (Fig. 1 and S3B†). These results indicate that (1) purification of PVP drastically inhibits the formation of Au NSTs, (2) aldehydes and pyridines in the PVP chain can reduce Au^{3+} to Au^{+}, (3) pyridines induce anisotropic growth, and (4) the presence of aldehydes in the PVP chain is not responsible for the formation of star-like NPs. Accordingly, no reaction was observed in attempts to produce NPs with PVP synthesized in our laboratory by conventional radical polymerization using 2,2′-azobisisobutyronitrile (AIBN) as an initiator (PVP-AIBN) (Fig. 1 and S3C†). Nevertheless, PVP-AIBN, which is –H terminated, is able to partially reduce Au^{3+} to Au^{+} (Fig. S3C†). Fig. S3D† displays the evolution of gold seeds into Au NSTs in the presence of impure PVP-TCI-10k by UV-Vis-NIR spectroscopy. After 90 minutes, the UV-Vis-NIR extinction spectra exhibit two LSPR bands centred at 546 nm (core mode) and 840 nm (tip mode), respectively. None of those bands were observed in the presence of PVP-TCI-OH, PVP-TCI-pyridine, PVP-AIBN (Fig. S3A, B and C†) or purified PVP-TCI-10k with rough spheres as the result of the synthesis. These results confirm the hypothesis that impurities in commercial PVPs are responsible for the formation of Au NSTs.

It is important to point out that these impurities are not present in the PVP we synthesized using AIBN (see ^{1}H-NMR spectrum in Fig. 2) as no Au NSTs were formed under these conditions (Fig. 1 and S3C†). In addition, the particles obtained in the presence of pyridines suggest that the substance responsible for the anisotropic growth is a compound with reduction activity present in PVP as an impurity.

The same experimental methodology was applied using commercial PVP with higher molecular weight (PVP-Sigma-40k, Lot WXBC7054V, $M_w = 40$ kDa), and the results show that the formation of very well-defined stars is drastically hindered after purification of the PVP. As seen for the PVP with lower molecular weight (PVP-TCI-10k), the purified PVP-Sigma-40k lacks oligomers, supporting the hypothesis that the substance responsible for the formation of stars is present in the PVP as an impurity (Fig. S4†).

Commercial PVP is mainly produced by radical polymerization in the presence of ammonia (which is used to synthesize *N*-vinylpyrrolidone and remains as a residual contaminant), and hydrogen peroxide as an initiator which leads to the formation of hydrazine as a by-product.[35] Meanwhile, hydrazine is commonly used as a reducing agent in the formation of spherical and anisotropic NPs, including branched NPs[36–40] and it is not formed during the synthesis of PVP when using AIBN as an initiator. Speculating that hydrazine might be the impurity responsible for the formation of Au NSTs, we attempted to synthesize Au NSTs using purified PVP-TCI-10k and purified PVP-Sigma-40k in the presence of hydrazine. Different concentrations of hydrazine (2.5–21.8 mM) were used to evaluate its role in anisotropic growth. As shown in the TEM micrographs and the UV-Vis-NIR spectra (Fig. 3), an increase in hydrazine from 2.5 mM to 10.9 mM leads to the formation of branched Au NPs in the presence of both purified PVPs, PVP-TCI-10k, and PVP-Sigma-40k. In the case of purified PVP-TCI-10k, Au NST are also produced at a higher concentration of hydrazine (21.8 mM), whereas star formation appears to become stifled in the case of purified PVP-TCI-40k. This latter result and the fact that the shape and the extinction spectra of Au NST produced in the presence of "as received" and "hydrazine spiked" PVP differ somewhat suggest that the mechanism leading to the formation of Au NSTs may be complex. It is also not clear that commercial PVP grades indeed include hydrazine as an impurity. Nevertheless, our data show clearly that the addition of hydrazine to purified PVPs has a significant influence and can promote the formation of Au NSTs. However, more experiments should be carried out to elucidate the mechanism, improve the yield of the synthesis, reduce the degree of polydispersity, and the stability of the NPs.

Conclusions

In this work, we demonstrated that the chemical supplier and inherent purity of PVP play a key role in the synthesis of Au NSTs. Depending on the supplier, we observed the formation of rough or sharp stars as well as a lack of well-defined Au NSTs. We also showed that the purification of the PVP drastically suppresses the anisotropic growth and that aldehyde groups in the PVP chain are not responsible for the formation of Au NSTs. Our data also show that the addition of hydrazine to PVPs can promote the formation of Au NSTs and mitigate the *absence* of impurities that appear otherwise to be necessary for their formation.

Conflicts of interest

There are no conflicts to declare.

Acknowledgements

This work was supported by the Swiss National Science Foundation through the National Center of Competence in Research Bio-Inspired Materials. The authors further acknowledge the support by the University of Fribourg and the Adolphe Merkle Foundation. LR-L acknowledges funding from FCT (Fundação para a Ciência e Technologia) for the Scientific Employment Stimulus Program (2020.04021.CEECIND). We thank Aaron Lee for proof-reading the manuscript, and Liliane Ackermann-Hirschi for her support in synthesis of the stars.

References

1 C. G. Khoury and T. Vo-Dinh, *J. Phys. Chem. C*, 2008, **112**, 18849.
2 X.-L. Liu, J.-H. Wang, S. Liang, D.-J. Yang, F. Nan, S.-J. Ding, L. Zhou, Z.-H. Hao and Q.-Q. Wang, *J. Phys. Chem. C*, 2014, **118**, 9659.
3 L. Rodríguez-Lorenzo, A. Garrido-Maestu, A. K. Bhunia, B. Espiña, M. Prado, L. Diéguez and S. Abalde-Cela, *ACS Appl. Nano Mater.*, 2019, **2**, 6081.
4 R. de la Rica and M. M. Stevens, *Nat. Nanotechnol.*, 2012, **7**, 821.
5 M. Bhamidipati, H.-Y. Cho, K.-B. Lee and L. Fabris, *Bioconjugate Chem.*, 2018, **29**, 2970.
6 A. Teixeira, L. J. Paris, F. Roumani, L. Diéguez, M. Prado, B. Espiña, S. Abalde-Cela, A. Garrido-Maestu and L. Rodriguez-Lorenzo, *Materials*, 2020, **13**, 1934.
7 A. S. D. S. Indrasekara, S. Meyers, S. Shubeita, L. C. Feldman, T. Gustafsson and L. Fabris, *Nanoscale*, 2014, **6**, 8891.
8 L. Rodríguez-Lorenzo, R. A. Álvarez-Puebla, I. Pastoriza-Santos, S. Mazzucco, O. Stéphan, M. Kociak, L. M. Liz-Marzán and F. J. García de Abajo, *J. Am. Chem. Soc.*, 2009, **131**, 4616.
9 Y. Wang, L. Polavarapu and L. M. Liz-Marzán, *ACS Appl. Mater. Interfaces*, 2014, **6**, 21798.
10 W. Ma, M. Sun, L. Xu, L. Wang, H. Kuang and C. Xu, *Chem. Commun.*, 2013, **49**, 4989.
11 J. Qian, C. Xing, Y. Ge, R. Li, A. Li and W. Yan, *Spectrochim. Acta, Part A*, 2020, **232**, 118146.
12 A. Kedia and P. S. Kumar, *J. Mater. Chem. C*, 2013, **1**, 4540.
13 N. Pazos-Perez, L. Guerrini and R. A. Alvarez-Puebla, *ACS Omega*, 2018, **3**, 17173.
14 S. Barbosa, A. Agrawal, L. Rodríguez-Lorenzo, I. Pastoriza-Santos, R. A. Alvarez-Puebla, A. Kornowski, H. Weller and L. M. Liz-Marzán, *Langmuir*, 2010, **26**, 14943.
15 S. Trigari, A. Rindi, G. Margheri, S. Sottini, G. Dellepiane and E. Giorgetti, *J. Mater. Chem.*, 2011, **21**, 6531.
16 N. El Amri and K. Roger, *J. Colloid Interface Sci.*, 2020, **576**, 435.
17 S. Jharimune, R. Pfukwa, Z. Chen, J. Anderson, B. Klumperman and R. M. Rioux, *J. Am. Chem. Soc.*, 2021, **143**, 184.
18 L. K. Mireles, M.-R. Wu, N. Saadeh, L. Yahia and E. Sacher, *ACS Omega*, 2020, **5**, 30461.
19 L. M. Liz-Marzán, C. R. Kagan and J. E. Millstone, *ACS Nano*, 2020, **14**, 6359.
20 P. S. Kumar, I. Pastoriza-Santos, B. Rodríguez-González, F. J. García de Abajo and L. M. Liz-Marzán, *Nanotechnol*, 2008, **19**, 15606.
21 A. Kedia and P. Senthil Kumar, *J. Phys. Chem. C*, 2012, **116**, 1679.
22 I. Pastoriza-Santos and L. M. Liz-Marzán, *Adv. Funct. Mater.*, 2009, **19**, 679.
23 K. M. Koczkur, S. Mourdikoudis, L. Polavarapu and S. E. Skrabalak, *Dalton Trans.*, 2015, **44**, 17883.
24 A. Kedia and P. S. Kumar, *J. Phys. Chem. C*, 2012, **116**, 23721.
25 L. Shao, A. S. Susha, L. S. Cheung, T. K. Sau, A. L. Rogach and J. Wang, *Langmuir*, 2012, **28**, 8979.
26 S. Atta, M. Beetz and L. Fabris, *Nanoscale*, 2019, **11**, 2946.
27 G. Maiorano, L. Rizzello, M. A. Malvindi, S. S. Shankar, L. Martiradonna, A. Falqui, R. Cingolani and P. P. Pompa, *Nanoscale*, 2011, **3**, 2227.
28 S. Abalde-Cela, P. Taladriz-Blanco, M. G. de Oliveira and C. Abell, *Sci. Rep.*, 2018, **8**, 2440.
29 A. Guerrero-Martínez, S. Barbosa, I. Pastoriza-Santos and L. M. Liz-Marzán, *Curr. Opin. Colloid Interface Sci.*, 2011, **16**, 118.
30 E. Ranucci, P. Ferruti, R. Annunziata, I. Gerges and G. Spinelli, *Macromol. Biosci.*, 2006, **6**, 216.
31 K. Raith, A. V Kühn, F. Rosche, R. Wolf and R. H. H. Neubert, *Pharm. Res.*, 2002, **19**, 556.
32 Y. Xiong, I. Washio, J. Chen, H. Cai, Z.-Y. Li and Y. Xia, *Langmuir*, 2006, **22**, 8563.
33 F. Haaf, A. Sanner and F. Straub, *Polym. J.*, 1985, **17**, 143.
34 I. Washio, Y. Xiong, Y. Yin and Y. Xia, *Adv. Mater.*, 2006, **18**, 1745.
35 Y. E. Kirsh, *Water Soluble Poly-N-Vinylamides: Synthesis and Physicochemical Properties*, John Wiley & Sons, Chichester, 1998.
36 G. H. Jeong, Y. W. Lee, M. Kim and S. W. Han, *J. Colloid Interface Sci.*, 2009, **329**, 97.
37 I. Pastoriza-Santos, A. Sánchez-Iglesias, B. Rodríguez-González and L. M. Liz-Marzán, *Small*, 2009, **5**, 440.
38 M. Maillard, S. Giorgio and M.-P. Pileni, *J. Phys. Chem. B*, 2003, **107**, 2466.
39 M. Sawczyk and R. Klajn, *J. Am. Chem. Soc.*, 2017, **139**, 17973.
40 A. F. Alvarez-Paneque, B. Rodríguez-González, I. Pastoriza-Santos and L. M. Liz-Marzán, *J. Phys. Chem. C*, 2013, **117**, 2474.